Proprietary Information on Pages 1 through 6
Withheld Pursuant to 10 CFR 2.390

Shielding RAIs

RAI 6-4:

Provide drawings with dimensions and allowable manufacturing tolerances in all drawings for the new (Type 4/5) basket designs.

The amendment incorporates two new basket designs (Type 4 and Type 5) to allow for storage of damaged and failed fuel compartments. The applicant provided drawings for the new basket types, however, these drawings do not include dimensions for the basket cells that are designated to hold damaged or failed fuel cans with end caps. Also, none of the drawings includes allowable manufacturing tolerances. Because the dimensions and associated tolerances are critical parameters for shielding analyses, the applicant needs to revise the drawings to include these data.

The staff needs this information to determine if the NUHOMS EOS spent fuel dry cask storage system design meets the regulatory requirement of 10 CFR 72.236(d).

***REVISED* RESPONSE TO RAI 6-4:**

Based on a follow-up conference call with the NRC on May 1, 2019, this response was revised to provide clarification about the use of end caps for damaged fuel and the use of FFCs for failed fuel, and to provide an explanation that the displacement of damaged fuel/end caps and failed fuel/FFCs are limited to short distances within the fuel compartment.

For clarification, damaged and failed fuel can only be stored in the Basket Type 4L under Amendment 1.

On Sheet 3 of *UFSAR D*rawing EOS01-1010-SAR, the minimum basket cell dimensions are given as a square dimension of 8.80 inches minimum; these basket cells are used to store intact as well as damaged *fuel with the use of end caps,* and failed fuel *with the use of a* failed fuel can*ister (FFC)*. This is specified on the drawing by Note 21:

“Damaged or failed fuel may be stored in the DSC, but shall not be loaded in the same DSC. Damaged Fuel shall require end caps (items 52, 53, 56, and 57). Failed fuel shall require a failed fuel canister (items 58 through 65).”

Clarifications have also been added on Sheet 9 of Drawing EOS01-1010-SAR (Revision 2D), to the damaged/failed fuel basket assembly exploded view, to illustrate the distinction between the top and bottom end caps and an FFC.

Damaged fuel end caps consist of a top end cap and a bottom end cap installed at both ends of the damaged fuel in the basket compartment. The manufacturing of the end caps is performed after the basket is fabricated, and is based on the as-built cell dimensions to ensure compliance with the 0.12-inch gap requirement between the end caps and the inside surface of the fuel compartment, as stated in Note 18 on *D*rawing EOS01-1010-SAR:

“The top and bottom end caps shall be installed in the fuel cells, *with* a maximum total gap of .12 verified all around (assuming *end caps* shifting), between inside surface of the fuel compartment and end caps body (items 53 and 57).”

Note 18 has been revised to change “lid” to “end caps” to provide additional distinction between the end caps used for damaged fuel and the FFC lid used for failed fuel, and also to delete the last sentence, which is inherent to the first part of the note.

The cavity length of the DSC is adjustable to match the length of the fuel to be stored. Therefore, because the damaged fuel length is the same as the intact fuel length, the damaged fuel and end caps displacement will be limited.

The FFCs consist of a liner (item 58), a bottom lid assembly (items 59 and 60) welded to the liner, and a top lid (items 62 and 63). FFC external dimensions are given as a square dimension of 8.63 inches on Sheet 13 of Drawing EOS01-1010-SAR, and may be adjusted to fit individual fuel compartments as stated in Note 26 of Drawing EOS01-1010-SAR. The top lid of the FFC is installed on top of the FFC in the pool during loading operations, and is tightly fit to the FFC liner with a minimum gap (on the order of 0.03 inch) between the liner and the top lid.

Furthermore, Note 35 has been revised to specify that the FFC length will be adjusted to maintain a 0.5-inch gap between the FFC top lid and the top of the basket. Because the distance between the top of the basket and the DSC lid is 0.9 inch, the displacement of the FFC lid will be limited to 1.4 inches. Therefore, the 4.25-inch length of the FFC top lid will ensure that the lid will not separate from the FFC liner.

*Regarding the criticality analyses, f*uel compartment width variation was analyzed in UFSAR Section 7*.4.2.*A Part 2: "Determination of Most Reactive Configuration – Fuel Assembly Width Variation." The results described in Table 7-14 show k_{eff} values for 8.76 and 8.96 inches and demonstrate that a compartment width of 8.76 inches results in a higher k_{eff}. The most reactive configuration was determined to be 8.76 inches. Even with the effects of manufacturing tolerances, the basket cell dimension does not go below the bounded analyzed value *of* 8.76 inches.

Furthermore, Note 8 on *Drawing* EOS01-1010-SAR states: "Inspect fuel compartments to verify minimum inside dimension. Inspection may be performed prior to assembly." This note ensures that the effects of plate stack-up at the current plate width does not result in any individual basket cell having dimensions smaller than the square dimension of 8.80 inches minimum. Therefore, regardless of the manufacturing tolerances, the inspected dimension will be greater than the design requirement.

For the shielding analysis, nominal values for slot thickness are justified in the analysis because of the built-in conservatism. Metal-matrix composite (MMC) poison plates (aluminum with boron carbide (B_4C) particulates) are used for criticality control. There are various levels of effective B-10 content for the baskets, which is adjusted for the fuel type. To provide for a bounding analysis, all MMC in both EOS DSCs is treated as pure aluminum at a slightly reduced density. This allows for full credit of the mass of aluminum to be taken for gamma shielding while maximizing the neutron dose rate external to the HSM. The description of this built-in conservatism in the model can be found in UFSAR Sections 6.3 and A.6.3.

There are various aluminum plate thicknesses in the basket. *The thinnest aluminum plate is modeled where aluminum plates are used in the MCNP basket model, which* is conservative as it reduces the overall *shielding* basket mass. Therefore, slight variations resulting from manufacturing tolerances are bounded by the overall conservatisms described above.

Additionally, UFSAR Chapter 6 (Shielding Evaluation) and Chapter 7 (Criticality Evaluation) also clearly indicate that no credit is taken for the failed fuel canister or any secondary containers. Therefore, the level of detail of the dimensions provided *o*n *D*rawing EOS01-1010-SAR for the basket components is adequate for the shielding and criticality analysis.

Regarding the axial fitting, the EOS-DSC is shortened in the shielding models so that there is no axial gap between the intact fuel and EOS-DSC. The EOS-TC models are also shortened so

that there is no axial gap between the EOS-DSC and EOS-TC. Dose rates provided in UFSAR Chapter 6 for intact fuels are conservatively increased, particularly at the top and bottom parts of the EOS-DSC, and bound all axial positions of intact fuel. Moreover, shielding analyses show that reconfiguration of damaged/failed fuel have a negligible effect on dose rates, and that dose rates computed for intact fuel may be used for DSCs with damaged/failed fuel.

Note 32 of Drawing EOS01-1010-SAR has been revised to correct the item numbers used to define the gap between the FFC liner and the FFC top lid on Sheet 14.

Application Impact:

No changes as a result of this RAI *in Amendment 1 Rev 3*.

Note 18 (Sheet 1), Note 32 (Sheet 14), Note 35 (Sheet 14) and Sheet 9 of Drawing EOS01-1010-SAR, Revision 2D were revised as described in the revised response.

RAI 6-5:

Revise the drawings to include dimensions and manufacturing tolerances for the NUHOMS® MATRIX design.

The applicant provided drawings for the NUHOMS® MATRIX design. However, these drawings do not include the width of the vent covers and there is no information on the manufacturing tolerances for any of the components. In particular, the dimensions and allowable manufacturing tolerances of the vent covers are important to shielding analyses.

The staff needs this information to determine if the NUHOMS EOS spent fuel dry cask storage system design meets the regulatory requirement of 10 CFR 72.236(d).

***REVISED* RESPONSE TO RAI 6-5:**

Based on a follow up conference call with the NRC on May 1, 2019, this response was revised to add a general tolerance to limit the maximum under-tolerance for concrete components.

The full dimensions of the *outlet* vent cover are given on Sheet 14 of *the* UFSAR *D*rawing MX01-5000-SAR, with supplemental information provided in Detail H-H *(Sheet 9).* The dimensions of the inlet and outlet *vent*s are given on Sheets 9 and 12 of the same drawing.

Note 32 of Drawing MX01-5000-SAR (Revision 0C) has been revised to add that the thickness of concrete members shall have a -1/2" maximum tolerance. Some features will have much tighter tolerances to accommodate fit-up concerns but in no case would it exceed -1/2".

The shielding analysis uses nominal dimensions because of the built-in conservatism of the calculation. *A concrete density of 138 pcf is used in the HSM-MX MCNP models, which is conservatively low compared to the nominal concrete density of 150 pcf. This assumption is sufficient to bound a concrete tolerance of -1/2" given the large concrete thicknesses employed in the design. Moreover, the reinforcing bars required to meet the structural loading requirements are not modeled. The absence of rebar yields conservative surface-averaged dose rates as the system is gamma-dominated. The front and rear supports, the heat shields, the embedments and any other installation hardware providing some additional shielding are not modeled. Additionally, all the metal-matrix composite (MMC) poison plates containing various levels of effective B-10 content are treated as pure aluminum at a slightly reduced density. This allows for full credit of the mass of aluminum to be taken for gamma shielding while maximizing the neutron dose rate external to the HSM-MX. Moreover, the thinnest aluminum plate is modeled where aluminum plates are used in the MCNP basket model, which reduces the overall basket shielding mass.*

In addition to these MCNP modeling conservatisms, dose rates are maximal in front of the inlet and outlet vents which are gamma radiation streaming paths not sensitive to bulk concrete tolerances. Dose rates at vents are much higher than dose rates on front, roof, rear and end side surfaces of the NUHOMS® MATRIX. Small deviations from nominal thicknesses will not affect the maximum dose rates presented Section A.6 of the UFSAR.

Application Impact:

Drawing MX01-5000-SAR*, Revision 0B was* revised *as described in the response in Amendment 1 Rev 3 .*

Drawing MX01-5000-SAR, Revision 0C has been revised as described in the response.

RAI 6-7:

Provide the burnup, initial enrichment, and cooling time (BECT) combination for the proposed spent fuel contents that represent the bounding source terms used to determine radiation dose rates. Alternatively, provide a list of BECTs to demonstrate that the source terms from these new contents to be authorized under Amendment 1 result in radiation dose rates that are within the design limits.

Paragraph 234(a) of 10 CFR Part 72 requires that the design of a spent fuel storage system meets the regulatory requirements of 10 CFR 72.236. For radiation protection, 72.236(d) states: "Radiation shielding and confinement features must be provided sufficient to meet the requirements in §§ 72.104 and 72.106." The applicant performed a shielding analyses based on source terms listed in Tables 6-14 to 6-19 of Amendment 1, Revision 1 of the Safety Analysis Report (SAR) for selected BECT combinations. In Section 6.2 of the SAR, the applicant states: "The bounding HLZCs are used for dose rate analysis" and that the source terms are developed to be "reasonably bounding consistent with the limits on fuel qualification." However, the maximum burnup and minimum cooling time parameters provided in the proposed Technical Specifications (TS) Table 2.1 does not include an associated minimal enrichment value and does not mirror the fuel parameters used in the calculation of the design basis radiation sources as shown in Tables 6-14 to 6-19 of Amendment 1, Revision 1 of the SAR. Without the associated minimal enrichment, the source terms for a fuel assembly with a given burnup and cooling time are not defined. Although the applicant provides the decay heat limits for the various loading patterns in the TS, there is no information provided on the specific relationship between the decay heat and the radiological source terms. A fuel assembly with a given decay heat can produce a wide variation of radiological source terms.

It is important to note that the recommendations published in NUREG/CR-6716, "Recommendations on Fuel Parameters for Standard Technical Specifications for Spent Fuel Storage Casks" are based on a balanced evaluation of parameters important to safety while alleviating limitations in the TS to provide the certificate of compliance holders flexibility to make design changes under the provisions in 10 CFR 72.48.

The staff requests this information to determine if the NUHOMS® EOS spent fuel dry cask storage system design with the requested new contents meets the regulatory requirements of 10 CFR 72.236(d).

***REVISED* RESPONSE TO RAI 6-7:**

This response has been modified in response to the NRC clarification calls conducted on May 1 and June 11, 2019.

RAI 6-7 is similar to RAI 6-6. As part of the RAI 6-6 response, it is demonstrated that:

1. The design basis source terms utilized are bounding for the new contents in Amendment 1 when following the burnup/enrichment *relationship* in UFSAR Table 6-7. This is demonstrated by considering ~1700 burnup/enrichment combinations per zone.

2. The number of *low-enriched* "outlier" fuel *(LEOF)* assemblies (fuel assemblies outside the burnup/enrichment combinations considered when developing design basis source terms) is a very small fraction of the spent fuel population (<0.5%). *LEOF* assemblies primarily affect the neutron source.

3. *LEOF* assemblies have essentially no effect on normal condition storage dose rates (72.104) or accident condition storage dose rates (72.106) because the storage system is gamma dominated. In any case, the site dose analysis used to demonstrate compliance with Technical Specifications (TS) 5.1.2 and 72.104 limits must consider outlier fuel assemblies, if present.

4. While *LEOF assemblies* are not expected to have an effect on transfer cask accident (72.106) dose rates due to their limited number, because the transfer cask accident dose rates are neutron dominated, the transfer cask accident dose rates are conservatively doubled to address this scenario. Exposure at the site boundary is <1% of the 72.106 dose limit.

The shielding analysis provided in the UFSAR is comprehensive. It is based on the bounding HLZC *4* and every location in the basket is filled with the *thermally* hottest allowed fuel. *However, to provide additional assurance that TS dose rate limits will be met, two fuel qualification tables (FQTs) have been added to the TS. These FQTs provide minimum cooling times as a function of burnup and enrichment for two specific decay heat values.*

The first FQT (TS Table 7B) is applicable to all PWR fuel to be stored in the EOS-37PTH DSC and is developed for fuel at 2.4 kW, which is the thermally hottest PWR fuel included in Amendment 1. All fuel to be loaded must meet TS Table 7B minimum cooling time requirements. Linear interpolation on the values in this table is performed within the range of burnup and enrichment to determine the minimum cooling time for fuel to be loaded. Note that the FQT is intended only to provide additional assurance that dose rate limits are met. The FQT is not intended to control decay heat, as fuel assembly decay heat is determined prior to application of the FQT.

A second FQT (TS Table 7C) is developed that is applicable only for the peripheral zone (zone 3) of HLZC 4 and HLZC 7. HLZC 4 and HLZC 7 have identical peripheral zones, with 1.6 kW fuel. The design basis HLZC used in the dose rate analysis bounds both HLZC 4 and HLZC 7. It is not credible that other HLZCs could result in dose rates approaching the TS limits. Linear interpolation is also performed for this FQT to obtain minimum cooling times.

The peripheral region (zone 3) of HLZC 4 or HLZC 7 accounts for 80% of the dose rate on the side of the EOS-TC125/135 and 95% of the dose rate at the vents of the EOS-HSM or HSM-MX. The inner zone of HLZC 4 contributes ~20% of the EOS-TC125/135 surface dose rate, primarily due to neutrons. However, because neutrons contribute little to vent dose rates in the storage configuration, the inner zone contributes only ~5% to EOS-HSM or HSM-MX vent dose rates. Therefore, applying a minimum cooling time only to the peripheral region effectively limits system dose rates.

The PWR minimum enrichments from UFSAR Table 6-7 have been added to the TS as Table 7A. This allows a clear method to identify fuel categorized as LEOF. Because cooling times in the FQTs are provided for the analyzed region, LEOF falls into the unanalyzed region of the FQTs where no cooling times are provided. Therefore, extrapolation into the LEOF region is acceptable to determine minimum cooling times. For the FQTs provided, linear extrapolation is acceptable because the relationship between cooling times and burnup or enrichment is linear, although other extrapolation methods could be employed. This extrapolation provides an additional penalty because minimum cooling times increase for lower enrichments.

Because LEOF could have elevated neutron sources, additional restrictions are placed on LEOF fuel. The peripheral region is limited to 4 LEOF. A minimum of three non-LEOFs shall circumferentially separate LEOFs within the peripheral region. There are no limitations on the number and location of LEOF stored in the inner basket locations. Based on historical data, LEOF is expected to be encountered at a rate of 1 per 200 fuel assemblies and in most cases would not have any effect on dose rates because only a limited number would typically be present within the DSC. The effect on transfer cask dose rates is not expected to exceed 5% even if multiple LEOFs are present. LEOF would have virtually no effect on storage dose rates because storage dose rates are gamma dominated.

The methodology used to qualify fuel for loading, with examples, is described in new UFSAR Section 6.5.1. The loading procedures in Chapter 9, Section 9.1.1, refer to TS Section 2.1 for radiological criteria.

TS Section 1.1 is modified to add a definition of LEOF. TS Section 2.1 is modified to add a method to identify LEOF (Table 7A) and loading restrictions for LEOF. TS Section 2.1 is modified to add an FQT for all fuel (Table 7B), and peripheral fuel in HLZC 4 and HLZC 7 (Table 7C). Footnotes are included below the FQT tables to provide guidance on use of the FQTs.

The footnotes to TS Figures 1B and 1C are modified to clearly indicate that minimum cooling times for fuel transferred in the EOS-TC108 is 3 years (larger in the peripheral zone), which is unchanged from Amendment 0.

Application Impact:

The TS has been revised as described in the *revised* response.

New UFSAR Section 6.5.1 has been added as described in the revised response.

RAI 6-8:

Provide justification for why the average rather than the peak side surface dose rate was used as a means to identify the bounding loading patterns.

On Page 6-9 of Amendment 1 Revision 2 of the SAR for the NUHOMS EOS system, the applicant states: “The bounding HLZCs are used for dose rate analysis.” On the same page, the applicant further states: “Based on MCNP scoping calculations, HLZC 4 bounds HLZC 1, and HLZC 4 and HLZC 5 result in similar peak dose rates for the EOS-TC1251135 and EOSHSM. However, HLZC 4 results in larger average dose rates on the EOS-TC125/135 side surface compared to HLZC 5 because HLZC 4 has the largest heat load in the peripheral zone. Therefore, HLZC 4 is used in design basis PWR calculations for the EOS-TC125/135 and EOSHSM. Source terms for HLZC 4 are derived for 1.0 kW/FA in Zone 1and1.625 kW/FA in Zones 2 and 3 for a total DSC heat load of 52. 0 kW. This bounds the maximum DSC heat load of 50. 0 kW.” The staff reviewed the heat load zone configurations HLZCs 4 and 5 and notes: (1) the fuel assemblies in HLZC 5, zone 3 are much hotter (3.4 kW) than those in zone 3 of HLZC 4, (2) the fuel assemblies in HLZC 5, zone 3 are not shielded by any fuel assemblies, and (3) HLZC 5 has an asymmetric loading pattern in terms of heat load. Therefore, HLZC 5 may have much higher dose rate at the some spots at the side where fuel with 2.4 kW decay heat is allowed. Also, the staff could not determine if the average dose rate can correctly identify the bounding loading pattern for dose rate calculations because of the asymmetric loading of HLZC 5. The SAR does not provide information on how the peak dose rate was calculated.

The staff needs this information to determine if the NUHOMS EOS spent fuel dry cask storage system design meets the regulatory requirement of 10 CFR 72.236(d).

***REVISED* RESPONSE TO RAI 6-8:**

This response has been modified in response to the NRC clarification call conducted on May 1, 2019.

The following methodology is used to determine EOS-TC125/135 source terms and dose rates:

1. *Burnup, enrichment, and cooling time (BECT) combinations with minimum enrichment according to UFSAR Table 6-7 are selected to target the decay heats used in the analyzed HLZCs. These BECT combinations are summarized in UFSAR Table 6-8. Source terms for a complete fuel assembly are available for every BECT in this table.*

2. *For the HLZC under consideration, the average dose rate around the circumference of the EOS-TC125/135 near the peak of the axial distribution is computed separately for each HLZC zone using MCNP. Each BECT combination in Table 6-8 is evaluated. Therefore, a bounding BECT is determined for each HLZC zone. <u>These average dose rates are used only to rank the BECT combinations.</u>*

3. *For the bounding BECT combinations, source terms are developed for the four source regions (bottom nozzle, active fuel, plenum, and top nozzle). All bounding source terms are provided in the UFSAR.*

4. *Dose rates are computed using a detailed MCNP tally structure that includes 24 angular segments and 18 axial segments around the body of the cask, as illustrated in UFSAR Figure 6-8 through Figure 6-10. Peak EOS-TC125/135 dose rates are reported in UFSAR Table 6-53.*

In response to this RAI, *bounding* source terms are developed for HLZC 5, and a*n explicit* dose rate analysis is performed for HLZC 5 to allow direct dose rate comparisons with HLZC 4 dose rates. It is demonstrated that HLZC 4 dose rates*, both peak and average,* bound HLZC 5 dose rates in the EOS-TC125/135. *Therefore, HLZC 4 is considered the design basis for EOS-TC125/135 analysis.* For the EOS-HSM, HLZC 4 and HLZC 5 result in similar vent dose rates. However, the design basis HLZC for EOS-HSM analysis is the EOS-89BTH DSC HLZC 1, which bounds PWR HLZC *4 and HLZC* 5.

UFSAR Chapter 6 has been revised to include HLZC 5 source terms and dose rates, primarily in Sections 6.2.2, 6.4.3, and 6.4.4. EOS-TC125/135 source terms are provided in Table 6-16d through Table 6-16g, and dose rates have been added to Table 6-53. EOS-HSM source terms are provided in Tables 6-19a through 6-19d, and vent dose rates are provided in Section 6.4.4.

As part of the revised response, some of the language related to the exposure analysis added to UFSAR Section 6.2.2 as part of the original response has been deleted.

Application Impact:

UFSAR Sections 6.2.2, 6.4.3, and 6.4.4 *were* revised as described in the response *in Amendment 1 Rev 3*.

UFSAR Tables 6-16d through 6-16g, 6-19a through 6-19d, and 6-53 *were* added as described in the response *in Amendment 1 Rev 3.*

UFSAR Section 6.2.2 has been revised as described in the revised response.

Proprietary Information on Pages 17 through 24
Withheld Pursuant to 10 CFR 2.390

Criticality RAIs

RAI 7-1:

Clarify Table 4 of the proposed Technical Specifications (TS) to clearly state which basket types are used for damaged/failed fuel.

Table 4 of the TS shows fuel loading parameters for damaged/failed fuel for all basket types. This is contradictory with the statements in the SAR and analyses in the SAR that state that damaged/failed fuel is only allowed for Basket Type 4. The applicant needs to provide justification to support the proposed TS Table 4 or clarify and revise the proposed TS if necessary to clearly state the basket types where damaged/failed fuel is allowed consistent with the SAR.

This information is needed in conjunction with 10 CFR 72.236(a).

***REVISED* RESPONSE TO RAI 7-1:**

Based on a follow-up conference call with the NRC on May 1, 2019, this response was revised.

Proposed Technical Specifications (TS), Table 4 indicates that pressurized water reactor (PWR) fuel can be stored in Basket Types A1/A2/A3/A4H/A4L/A5 as well as B1/B2/B3/B4H/B4L/B5. However, distinction should be made to indicate that only Basket Types A4L and B4L can store damaged and failed fuel. As such, new notes 2 and 3 are added to Table 4 of the TS to clarify that damaged and failed enrichments can only be loaded in Basket Types A4L and B4L, respectively.

The table on UFSAR Page 1-2 has been revised for clarification. A note *has also been* added on Page 7-1 *for clarification. Table 7-51 has been deleted and replaced by a reference to Table 4 of the TS for convenience.*

These changes do not affect the enrichments for the EOS-37PTH DSC damaged/failed fuel, but ensure consistency with the system configurations for the EOS-HSM and HSM-MX systems shown in Table 1-2 of Chapter 1.

UFSAR Reference 7-7 is changed to the updated reference of the CoC 1004, UFSAR Revision 16. This change is just an editorial change.

Application Impact:

UFSAR Chapter 7, Section 7 and Table 7-51 *were* revised *as described in the response in Amendment 1 Rev 3, and subsequently revised as described in the revised response*.

UFSAR Section 1.1 has been revised as described in the response.

TS Table 4 *was* revised *as described in the response in Amendment 1 Rev 3, and subsequently revised as described in the revised response*.

Proprietary Information on Pages 26 through 38
Withheld Pursuant to 10 CFR 2.390

RAI 8-6:

Provide the following additional information for UFSAR Tables A.8-2, A.8-3 and A.8-4 which apply to ASTM A572 Grade 50, ASTM A992 Grade 50, and ASTM A588 steels respectively:

1. Justify the methodology used to estimate the mechanical properties of these steels atelevated temperatures.

   There are several established methodologies used to estimate the elevated temperature mechanical properties of structural steel. Sief et al., (2016) reviewed elevated temperature properties for structural steels and compared the estimated values from several models to actual data for the elastic modulus, yield strength and tensile strength (NIST Technical Note 1907 Figures 2-3, 2-4 and 2-6 respectively). Sief et al., (2016) showed significant variations in the mechanical properties of structural steels as well as variations in the predicted values of models used to estimate the mechanical properties at elevated temperatures.

   Aziz and Kodur (2016) also showed significant differences between predicted values and actual measured values of yield strength and elastic modulus for ASTM A572 Grade 50 at elevated temperatures.

2. Provide allowable stress values for these materials as a function of temperature, a technical basis for the determination of the allowable stresses and an analysis showing that the actual stresses do not exceed the allowable stresses.

   Tables A.8-2, A.8-3 and A.8-4 for ASTM A572 Grade 50, ASTM A992 Grade 50, and ASTM A588 steels, respectively, contain information on the predicted values of yield and tensile stresses and elastic modulus. Allowable stresses for these materials are not provided and the analyses conducted do not include an assessment of the actual stresses compared to the allowable stresses as a function of temperature.

This information is needed to determine compliance with 10 CFR 72.236(b).

***REVISED* RESPONSE TO RAI 8-6:**

Based on a follow up conference call with the NRC on May 1, 2019, this response was revised as follows:

- *The temperature-dependent reduction factors for the mechanical properties of the all three steels discussed in this RAI, namely, ASTM A572 Grade 50, ASTM A992 Grade 50, and ASTM A588, are based on UFSAR Reference A.8-8 [1]. It is demonstrated that the use of the reduction factors from [1] leads to a conservative structural evaluation compared with the use of the factors from different sources, such as NIST [2], Aziz and Kodur [3], and AISC [4].*

- *A discussion is provided to emphasize that the AISC specification [4], like other design codes, accounts for the variability of the strength of the structural members through the use of safety factors, and additional safety factors for the variability of mechanical properties at elevated temperatures are not necessary. Comparisons of the allowable stresses based on AISC [4] and ASME BPVC [5] are presented to demonstrate the similarities of the requirements by the two codes.*

Response to Part 1

As shown in UFSAR Table A.8-1, ASTM A572 Grade 50, ASTM A992 Grade 50, and ASTM A588 steels are used for the HSM-MX DSC support pedestal/stop plate, DSC support pedestal, and axial retainer rod, respectively. As indicated in the footnotes of UFSAR Tables A.8-2*,* A.8-3, *and A.8-4,* the mechanical properties at elevated temperatures for *the three* steels are calculated using the rate of reduction provided in the UFSAR Reference A.8-8 [1]. The rate of reduction *from Figures 7-3 and 7-4 of [1]* was applied to the room temperature values of the yield and ultimate strength*, respectively,* provided in the respective ASTM specification for *the three steels*. Similarly, the rate of reduction *from Figure 7-5 of [1]* was applied to the *room temperature value of the* modulus of elasticity provided in *AISC (= 29,000 ksi)* [*4*]*, which is applicable for all three steels*.

Figure*s RAI 8-6*-1, *RAI 8-6*-2, and *RAI 8-6*-3 show *four* temperature-dependent reduction factors *based on the following four different sources,* for the elastic modulus (*E*), yield strength (F_y), and tensile strength (F_u), respectively *(Note that for temperatures up to 700 °F, 250 °F is the bounding temperature for the HSM-MX DSC support pedestal/stop plate and axial retainer rod for the normal and off-normal conditions (UFSAR Figures A.4-21 and A.4-22))*:

- Temperature-dependent reduction factors *used in the UFSAR analyses* for ASTM A572 Grade 50*,* ASTM A992 Grade 50*, and ASTM A588* (based on *Figures 7-5, 7-3, and 7-4 of* UFSAR Reference A.8-8 [1] *for E, F_y, and F_u, respectively*)*,*

- Proposed temperature-dependent reduction factors from NIST Technical Note 1907 *[2]* (Equations 2.2, 2.4, and 2.14 of [2] for *E, F_y, and F_u,* respectively)*,*

- Proposed temperature-dependent reduction factors by Aziz and Kodur [3] (Equations 1, 2, and 3 of [3] for *E, F_y, and F_u,* respectively)*, and*

- *Temperature-dependent reduction factors provided in AISC [4] (Table A-4.2.2)*

Figure *RAI 8-6*-1 shows that the temperature-dependent values of modulus of elasticity used in the UFSAR are in very good agreement with those from NIST Technical Note 1907 [2], but greater than those from Aziz and Kodur [3] throughout the entire temperature range. *The UFSAR modulus of elasticity is slightly lower than the AISC [4] values for the temperature lower than 250 °F, but higher above 250 °F.* Figure *RAI 8-6-2* shows that the temperature-dependent values of yield strength used in the UFSAR are less than those from NIST [2]*,* Aziz and Kodur [3]*, and AISC [4]* for the entire temperature range, with the exception that the UFSAR *values* are slightly greater than those from NIST [2] for *a very high temperature range (> 600 °F)*. Figure *RAI 8-6*-3 shows that the temperature-dependent values of tensile strength used in the UFSAR are in good agreement with those from NIST [2]*,* Aziz and Kodur [3]*, and AISC [4]* for temperature*s less than 400 °F*. *Since 250 °F is the bounding temperature considered in the structural evaluations of the HSM-MX components made of the three steels, those observations made above for temperatures greater than 250 °F have no implications in this response.*

*Of the observations made on the comparison of the temperature-dependent reduction factors from different sources, the most significant, for the purpose of the structural evaluation of the components made of the three steels, is that the yield strength used in the UFSAR is less than those from all the other sources for the temperature under 600 °F. The reason is that s*tructural evaluations of the HSM-MX DSC support pedestal/stop plate and axial retainer rod use the tensile, compressive, and shear strengths of the materials*, which primarily depend on the yield strength*. *For the structural evaluations, t*he material properties at 250 °F *are used*, which is the bounding temperature for the HSM-MX DSC support pedestal/stop plate and axial retainer rod, for the normal and off-normal conditions.

- The tensile and shear strengths rely on the yield strength. As shown in Figure *RAI 8-6-2*, the yield strengths used in the UFSAR are less than those proposed by NIST [2]*,* Aziz and Kodur [3], *and AISC [4] for the temperature under 600 °F .* Therefore, the mechanical property values used in the UFSAR for the tensile and shear strengths are conservative.

- The compressive strength relies on both the yield strength and modulus of elasticity. According to the AISC steel construction manual [4], the critical stress F_{cr} for compressive strength*, for* $KL/r \le 4.71\sqrt{(E/F_y)}$*,* is:

  $F_{cr} = [0.658^{(Fy/Fe)}]F_y$

  where $F_e = \pi^2E/(KL/r)^2$ and KL/r is the effective slenderness ratio. As shown in Figure *RAI 8-6-*4, the critical stress for KL/r of 34.4, which was used in the *UFSAR* evaluation of the HSM-MX DSC support pedestal, is less than those proposed by NIST [2]*,* Aziz and Kodur [3]*, and AISC [4]* for the temperature *under 600 °F*. Therefore, the mechanical property values used in the UFSAR for the compressive strength are conservative.

The discussion presented above demonstrates that the mechanical properties for the ASTM A572 Grade 50, ASTM A992 Grade 50, and ASTM A588 steels presented in UFSAR Tables A.8-2, A.8-3 and A.8-4 are conservative when compared with the properties proposed in the recent publications ([2] and [3]) *and AISC [4]*. *In particular, the allowable yield strength and critical stress at 250 °F used in the UFSAR analyses are less by about 10% than those due to AISC [4], which is the design code for the HSM-MX steel components.* Therefore, the methodologies used to estimate these properties are appropriate.

As a result of this revised RAI response for Part 1, UFSAR Tables A.8-2, A.8-3, and A.8-4 have been revised, with the temperature-dependent reduction factors from [1] being applied to the room temperature values of the yield and ultimate strength provided in the ASTM specifications and to the room temperature value of the modulus of elasticity provided in AISC [4], for ASTM A572 Grade 50, A992 Grade 50, and A588 steels.

Response to Part 2

Since the allowable tensile *and* shear stresses are directly related with the yield strength, their temperature-dependent variations *follow the same curve, which is shown in Figure RAI 8-6-2*. *Similarly, since the allowable compressive stress is directly related to F_{cr}, its temperature-dependent variation also follows the same curve as shown in Figure RAI 8-6-4.* As demonstrated in the response to Part 1 of this RAI, these properties are based on conservative estimations of the mechanical properties for the *three* steels at elevated temperatures.

Structural evaluation of the DSC support pedestal/stop plate (A572/A992): The maximum load in the DSC longitudinal direction and the maximum compressive load on the DSC support are 135.3 kips and 156.5 kips, respectively. The evaluations for the DSC support Option A*, which result in the highest demand-to-capacity ratio, are shown below*.

- Shear of the rear DSC support stop plate: The *allowable* shear strength based on the yield strength of 45 ksi at 250 °F is 249.0 kips > 135.3 kips (Therefore, this is acceptable.)

- Connection between the stop plate and top flange of the W-beam: The connection *allowable* strength based on the yield strength of 45 ksi at 250 °F is 164.5 kips > 135.3 kips (Therefore, this is acceptable.)

- Web shear in the W-beam: The shear strength based on the *allowable* yield strength of 45 ksi at 250 °F is 157.3 kips > 135.3 kips (Therefore, this is acceptable.)

- Compression of the W-beam: The *allowable* compressive strength based on the yield strength of 45 ksi and modulus of elasticity of 28,1*00* ksi *at 250 °F* is 156.9 kips > 156.5 kips (Therefore, this is acceptable.)

Structural evaluation of the axial retainer rod (A588): The maximum load in the DSC longitudinal direction is 270.5 kips.

- Compression of the axial retainer rod: The compressive strength based on the yield strength of 45 ksi and modulus of elasticity of 28,*100* ksi *at 250 °F* is 280.3 kips > 270.5 kips (Therefore, this is acceptable.)

The UFSAR analyses use the AISC code, which contains safety factors as required by any design codes. These safety factors account for the variability of the strength of the structural members, which includes the variability in the material mechanical properties. These safety factors are compared with the ASME BPVC safety factors below and summarized in Table RAI 8-6-1.

For example, the Level A allowable tensile stress for linear-type supports specified by the ASME BPVC (NF-3322 of [5]) is $F_t = 0.60S_y$, where S_y is the yield strength. The Service Level D stress limit factor, according to Appendix F-1334 of [6], is the smaller of 2 or $1.167S_u/S_y$ if $S_u > 1.2S_y$, or 1.4 if $S_u \leq 1.2S_y$. Since $S_u > 1.2S_y$ for A572 / A992 at 250 °F, the stress limit factor is min(2, $1.167S_u/S_y$) = min(2,1.67) = 1.67, resulting in the Level D (seismic) allowable tensile stress of $1.67F_t = 1.00S_y$. In addition, per Section F-1334.1 of [6], the Level D allowable tensile stress is the lesser of $1.2S_y$ and $0.7S_u$. For A572 / A992, $0.7S_u \geq 1.00S_y$ at 250 °F. Therefore, the Level D allowable tensile stress is $1.00S_y$.

On the other hand, the allowable tensile strength specified by the AISC code (Section D2 of [4]) is F_yA_g/Ω, where F_y is the yield strength (= S_y), A_g is the gross cross-sectional area, and Ω is the safety factor (= 1.67). Therefore, the allowable tensile stress is $F_y/\Omega = 0.60F_y$, and the allowable tensile stress for seismic load, which includes the strength increase factor of 1.6 for tension (UFSAR Table 3.9.4-16), is $1.6F_y/\Omega = 0.958F_y$. It is seen that the allowable stresses specified by the AISC code contain built-in safety factors like those in accordance with the ASME BPVC.

The safety factors inherent in the ASME BPVC are demonstrated in Figure 2 of [8], as shown in Figure RAI 8-6-5, which compares the design limits to the limit stress for tension and bending. As supported by the analysis above, these safety factors are shown to be between 1.5 and 1.7 for tension plus bending, and 1.5 for tension. Similar safety factors are expected for the AISC criteria.

Therefore, once the material properties are established based on published data, no additional safety factors are required. In addition:

- *The temperature-dependent reduction factors for the mechanical properties employed in the UFSAR analysis are conservative as demonstrated in Part 1 of this RAI.*

- *The structural evaluations performed to qualify these components include conservatisms. For example, in the evaluation for the compression of the W-beam, when the buckling strength of the web is computed, the lateral restraint along the length of the member is conservatively ignored.*

Therefore, the actual safety margins in the structural evaluations of the components will be higher when compared with the values presented above.

References

[1] Mark Fintel, “Handbook of Concrete Engineering”, Second Edition, September 1985.

[2] NIST Technical Note 1907, “Temperature-Dependent Material Modeling for Structural Steels: Formulation and Application.”

[3] E. M. Aziz and V. K. Kodur, “Effect of temperature and cooling regime on mechanical properties of high-strength low-alloy steel,” Fire and Materials, Vol. 40, pp. 926-939, 2016.

[4] American Institute of Steel Construction, “AISC Manual of Steel Construction,” 13th Edition or later.

[5] *American Society of Mechanical Engineers, Boiler & Pressure Vessel Code, Section III, Division 1, Subsection NF, “Supports,” 2010 Edition with 2011 Addenda.*

[6] American Society of Mechanical Engineers, Boiler & Pressure Vessel Code, Section III, Division 1, Appendices, 2010 Edition with 2011 Addenda.

[7] American Institute of Steel Construction, “AISC Manual of Steel Construction – Allowable Stress Design,” 9th Edition.

[8] The American Society of Mechanical Engineers, “Criteria of the ASME Boiler and Pressure Vessel Code for Design by Analysis in Sections III and VIII, Division 2,” 1969.

Application Impact:

No changes as a result of this RAI *in Amendment 1 Rev 3.*

UFSAR Section A.8.7 has been revised as a result of this revised RAI response.

UFSAR Tables A.8-2, A.8-3, and A.8-4 have been revised as a result of this revised RAI response.

Table 8-6-1
Comparison of AISC and ASME allowable tensile stress values for ASTM A572 Gr. 50

Service Level	***ASME BPVC Section III, Subsection NF***	***AISC [Section D2]***
Level A	$F_t = 0.60S_y$ *[NF-3322]*	$F_t = F_y A_g / \Omega$ $F_t = 0.60F_y$
Level D	*Stress limit factor (SLF):* *For* $S_u > 1.2S_y$, $\min(2, 1.167S_u/S_y)$ *For* $S_u \leq 1.2S_y$, *1.4* *Allowable tensile stress:* $F_t = \min(SLF \times 0.60S_y, 1.2S_y, 0.7S_u)$ *[Appendix F-1334]* $F_t = 1.00\ S_y$	$F_t = 1.6F_y / \Omega$ $F_t = 0.958F_y$

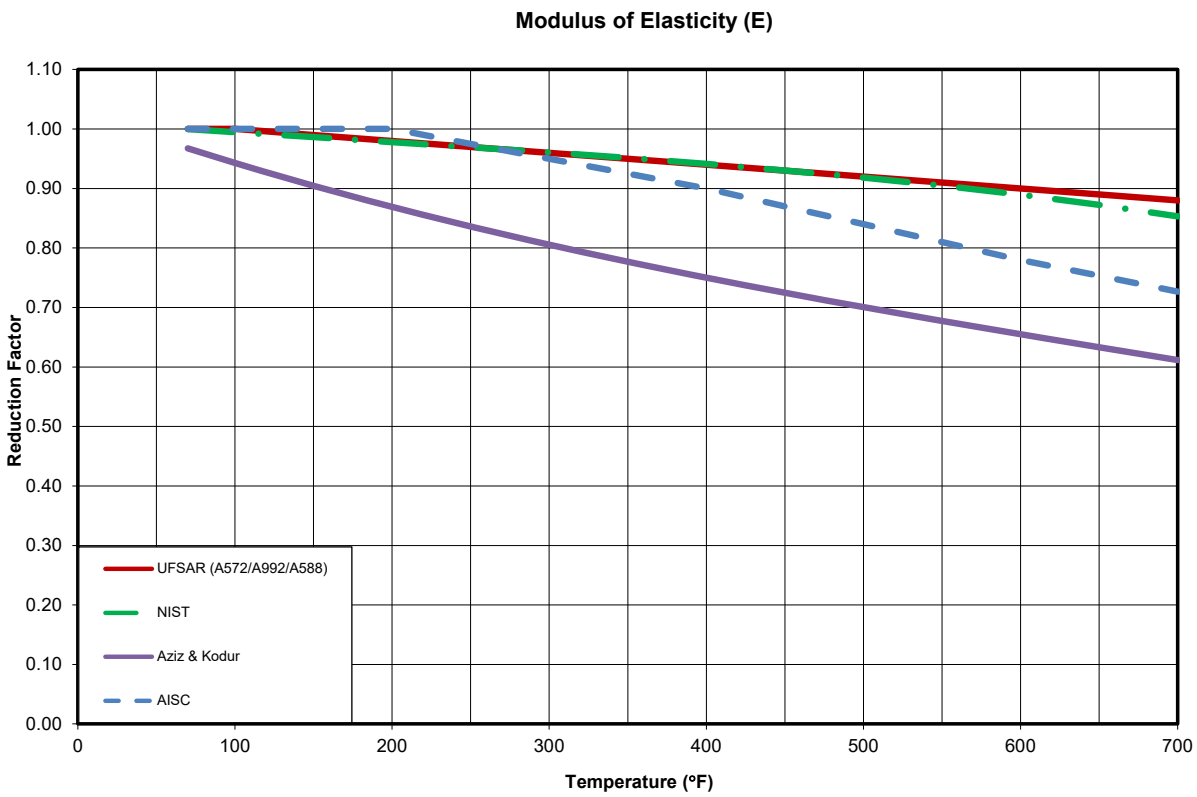

Figure *RAI 8-6-1*
Reduction factors for modulus of elasticity at elevated temperatures

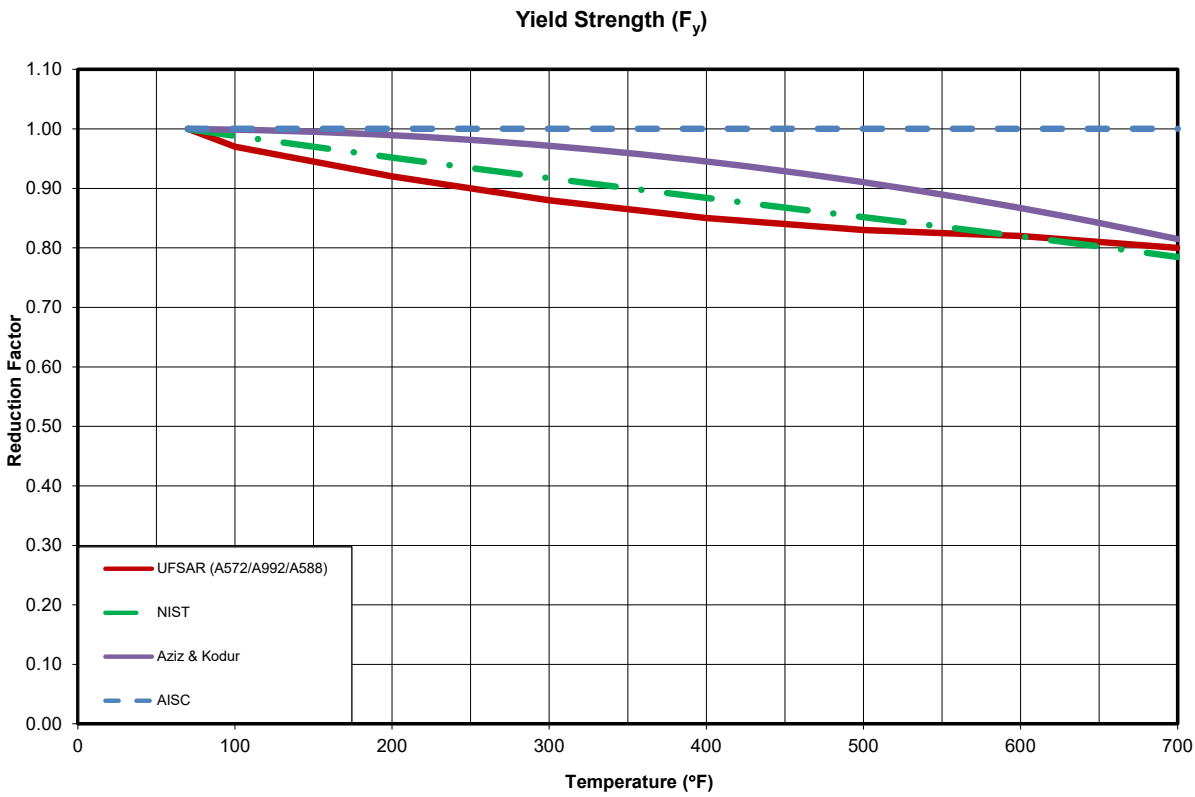

Figure *RAI 8-6-2*
Reduction factors for yield strength at elevated temperatures

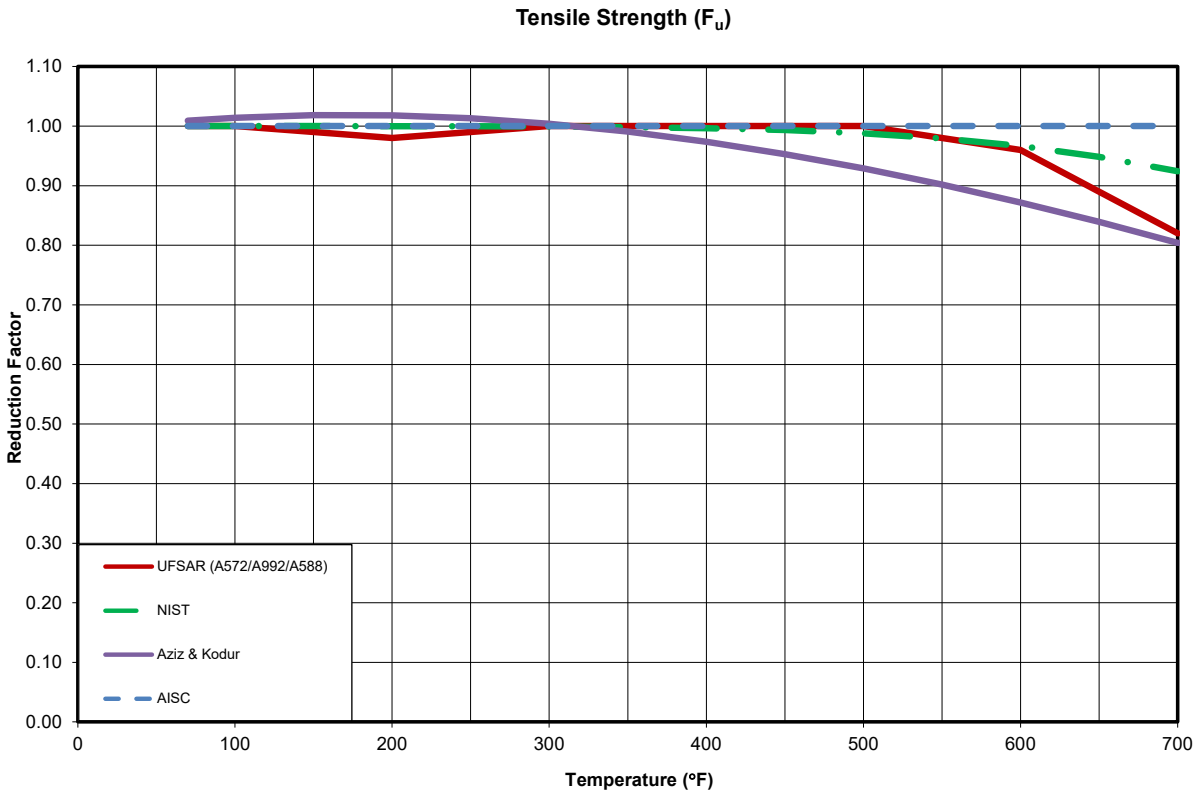

Figure *RAI 8-6-3*
Reduction factors for tensile strength at elevated temperatures

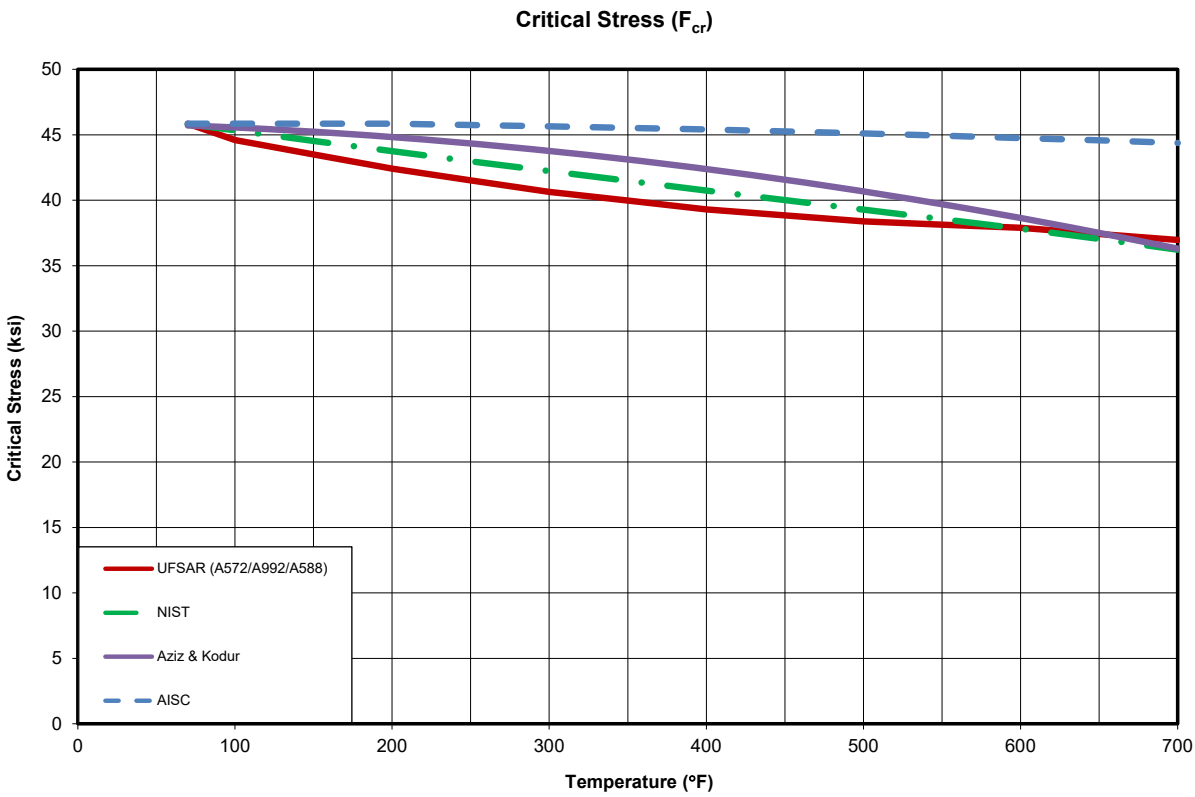

Figure *RAI 8-6-4*
Critical stress at elevated temperatures

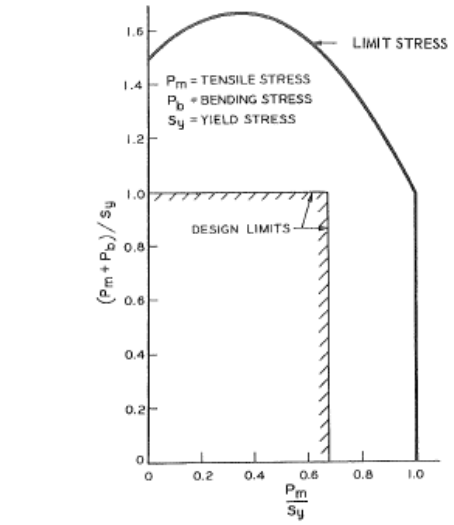

FIGURE 2. LIMIT STRESS FOR COMBINED TENSION AND BENDING (RECTANGULAR SECTION)

Figure RAI 8-6-5
Limit stress for combined tension and bending in ASME BPVC Sections III and VIII [8]

RAI 8-7:

Provide allowable stress values for ASTM A829 Gr 4130, AMS 6345 SAE 4130 and other HSLA steels as a function of temperature, a technical basis for the determination of the allowable stresses and an analysis showing that the actual stresses do not exceed the allowable stresses. ASTM A829 Gr 4130 or AMS 6345 SAE 4130 and other HSLA steels are identified in UFSAR Section 10.1.7. UFSAR Table 8-10 contains information on the predicted values of yield and tensile stresses and elastic modulus. Allowable stresses for these materials are not provided and the analyses conducted do not include an assessment of the actual stresses compared to the allowable stresses as a function of temperature.

This information is needed to determine compliance with 10 CFR 72.236(b).

***REVISED* RESPONSE TO RAI 8-7:**

UFSAR Table 8-10 provides the allowable stress values for ASTM A829 Gr 4130, AMS 6345 SAE 4130 and other *high strength low alloy (*HSLA*)* steels as a function of temperature based on the initial scoping analysis, which provides a yield stress (S_y) value of 80 ksi @ 500 °F that would provide sufficient margin when evaluating the design as described in Appendix.3.9.2. Based on the yield stress value of 80 ksi @ 500 °F, the rate of reduction provided in Figure 2.3.1.1.*1* of military handbook reference document, MIL-HDBK-5J, "Metallic Materials and Elements for Aerospace Vehicle Structures," U.S. Department of Defense Handbook, 31 January 2003, was utilized to derive temperature-dependent properties for the yield stress.

Similarly for Modulus of Elasticity (E), the value of 29.0 E +06 @ 70 °F is taken from Table *2.3.1.0 (c_1 through c_4) and Table 2.3.1.0 (g_1 and g_2)* of military handbook reference document, MIL-HDBK-5J, "Metallic Materials and Elements for Aerospace Vehicle Structures," U.S. Department of Defense Handbook, 31 January 2003. The rate of reduction from Figure 2.3.1.1.4 was utilized to derive the temperature-dependent properties for the Modulus of Elasticity.

The values for ultimate stress (S_u) are calculated conservatively to be low, assuming 1.05 * yield stress (S_y).

To validate the values provided in UFSAR Table 8-10, material testing was performed to meet or exceed the allowable limits as provided in reference Document No. 51-9230070, "Evaluating Optimum Tempering Temperature for AISI 4130 to achieve desired strength and toughness properties." A copy of this proprietary document is provided as Enclosure 14.

Reference Document No. 51-9230070, Table 5-1 provides the mean and lower bound yield stress values and Table 5-2 provide the mean and lower bound tensile stress values. Based on the material qualification as described in this document, ASTM A829 Gr 4130 or AMS 6345 SAE 4130, the lower bound yield and ultimate values (tested @ 70 °F) are 103.6 ksi and 123.1 ksi, respectively, as discussed in UFSAR Section 10.1.7. These test values exceed the design basis allowable values of yield and ultimate stress of 96.4 ksi and 101.2 ksi @ 70 °F, respectively, as provided in Table 8-10.

The structural analyses were performed in Appendix 3.9.2 based on the material properties provided in UFSAR Table 8-10 and results show that the calculated stresses meet these material allowable limits. To additionally ensure that these values are met, the material procured to fabricate the basket shall meet or exceed the allowable limits of 103.6 ksi and 123.1 ksi as discussed in in UFSAR Section 10.1.7.

Based on a follow up conference call with the NRC on May 1, 2019, for a clarification on why compressive yield strength was used, the RAI response has been revised to correct the typographical error: change Figure 2.3.1.1.2 to Figure 2.3.1.1.1, "Effect of temperature on the tensile ultimate strength and tensile yield strength of AISI low-alloy steel (all products)". The material properties value provided in UFSAR Table 8-10 remains valid based on UFSAR Figure 2.3.1.1.1.

The RAI response is also revised to correct the typographical error for the Young's Modulus value of 29.0 E +06 as provided in Section 2.3.1 to Table 2.3.1.0 (c_1 through c_4) and Table 2.3.1.0 (g_1 and g_2) per MIL-HDBK-5J.

The material qualification and production acceptance tests for HSLA steels, ASME SA-517 Gr. A, B, E, F, or P, and other HSLA steels are presented in the flow chart in Figure RAI 8-7-1 in support of this response.

The material qualification testing for other HSLA steels as described in UFSAR Section 10.1.7.C shall be performed using similar methodology to that applied to HSLA steel ASTM A829 Gr. 4130 or AMS 6345 SAE 4130 (Section 10.1.7.A) as described in the Reference Document No. 51-9230070 [8-7.1] to determine the temperature dependent properties. This is summarized in Section 10.1.7.C.i-iii.

For other HSLA steel, production acceptance testing will be performed at room temperature based on acceptance criteria determined by qualification testing using a similar methodology as that documented in Document No. 51-9230070 for AISI 4130 material. The 95% lower tolerance limit of yield and ultimate strength values for production acceptance testing are to be greater than or equal to the design values used in the UFSAR analysis as presented in Table 8-10. Technical Specifications Section 4.3.2 and UFSAR Section 10.1.7 have been revised to include production acceptance test criteria at room temperature for other HSLA.

References:

1. Enclosure *14* to CoC 1042, Amendment *1 Rev. 3,* AREVA Inc. Document No. 51-9230070-000, "Evaluating Optimum Tempering Temperature for AISI 4130 to Achieve Desired Strength and Toughness Properties".

Application Impact:

No changes as a result of this RAI *in Amendment 1 Rev 3*.

Enclosure 14 has been provided *as described in the response in Amendment 1 Rev 3*.

UFSAR Section 10.1.7 has been revised as described in the response.

Technical Specifications 4.3.2 has been revised as described in the response.

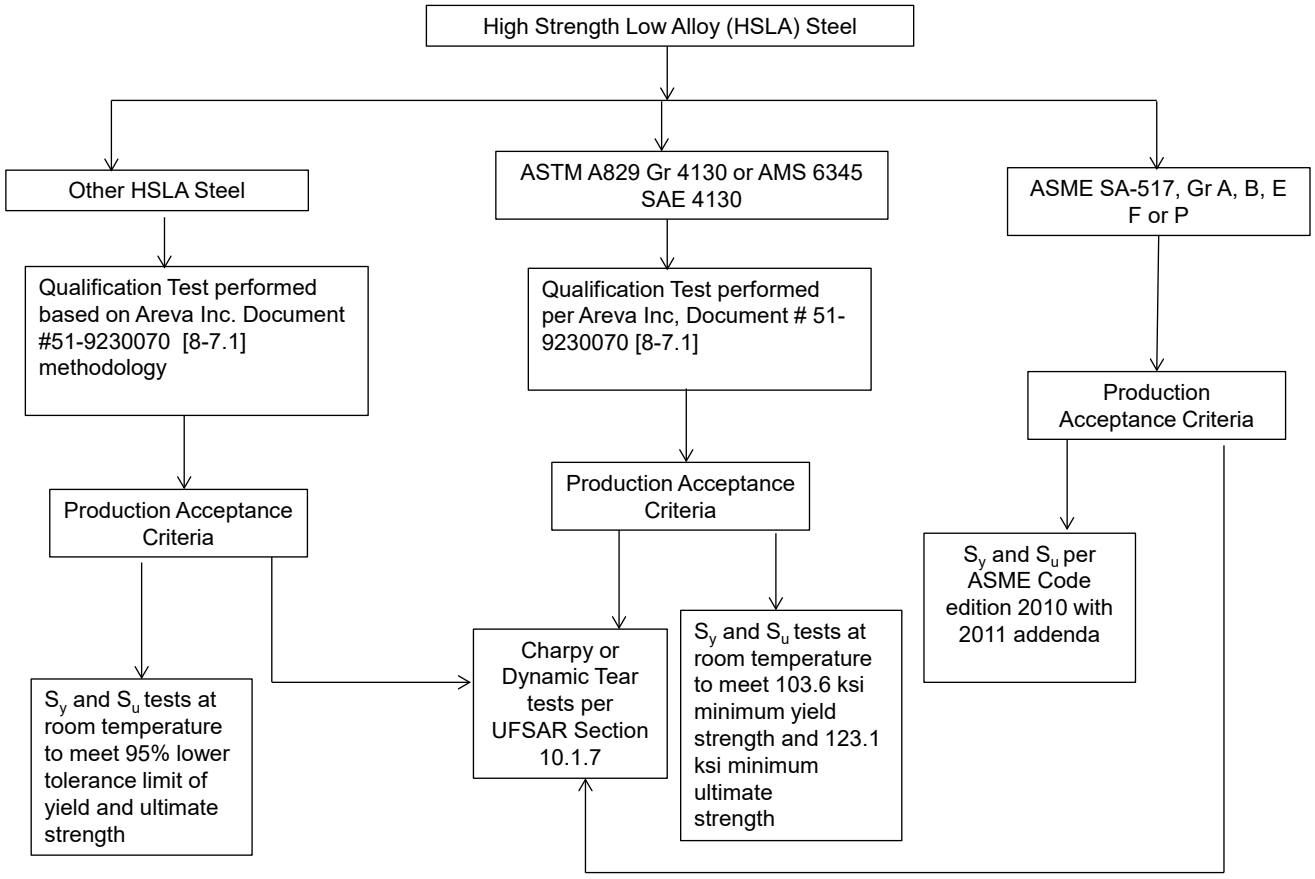

Figure RAI 8-7-1
HSLA Steel Qualification and Acceptance Tests

Operating Procedures RAIs

RAI 9-2:

Provide the following information on the fuel spacers identified in UFSAR Amendment 1 Revision 0 Section 9.1.1 Steps 1.b. and 9.b.:

1. Clarify whether the evaluation for adverse impact of the fuel spacers is related to Part 72 activities or Part 71.

   Section 9.1.1 Step 1.b of Amendment 1 Revision 0 of the NUHOMS EOS System UFSAR, states, in part, " ... There are no requirements for fuel spacers under Part 72. Fuel spacers, if used, may be placed below the assembly, above the assembly, or both, and shall be evaluated for any adverse impact." It is unclear whether the adverse impact is in reference to storage or transportation operations.

2. Clarify the use of the term "requirements" in the above mentioned statement in UFSAR Section 9.1.1 Step 1.b and the term "required" in the description provided in UFSAR Section 9.1.1 Step 9.b. Section 9.1.1 Step 9.b of Amendment 1 Revision 0 of the UFSAR states, in part,

   "... verify that the bottom fuel assembly spacers, if required, are present in the fuel cells." It is unclear if the fuel spacers identified on UFSAR pages 9-3 and 9-4 are the same component or if the term "fuel spacers", that may be required, on page 9-4 refers to a different component than the item identified on USFAR page 9-3.

3. Provide drawings with dimensions, allowable manufacturing tolerances, material specifications, quality category and code criteria for the fuel spacers identified in UFSAR Chapter 9 Section 9.1.1.

   The application contains two changes to UFSAR Section 9.1.1 which identify the use of fuel spacers in step 1.b. and step 9.b. Based on the context of the changes in UFSAR Section 9.1.1, it appears that there is more than one type of spacer that may be used in the EOS DSCs. The drawings provided by the applicant do not appear to include specific information on the fuel spacers identified in Section 9.1.1 Steps 1.b. and 9.b.

The staff needs this information to determine if the NUHOMS EOS spent fuel dry cask storage system design meets the regulatory requirement of 10 CFR 72.236(a), (b), (c), (d), (f) and (h).

***REVISED* RESPONSE TO RAI 9-2:**

Response to Part 1:

The EOS DSCs are designed to be variable in length as to minimize the need for fuel spacers. However, the need for fuel spacers arises when various types of control components are stored, such that even within a DSC, not all fuel assemblies are the same length. For the EOS-89BTH, the DSC is sized such that fuel spacers are not needed.

The fuel spacers replace the void at the top or bottom of a fuel assembly to reduce the gap between the fuel assembly and the DSC cavity to mitigate the effect of impact for the drop accidents for transportation under 10 CFR Part 71. Their purpose is to maintain a minimum nominal gap requirement between the fuel and the *DSC cavity in order to* avoid adverse effects, including damage to the fuel assembly, rods, or cladding, due to a secondary impact under transport accident conditions. The transport cask is licensed under the 10 CFR Part 71.

Response to Part 2

The clarification provided in the response to RAI 9-2 Part 1, above, has been added to UFSAR Section 9.1.1, Step 1.b.

The fuel spacers referenced in Section 9.1.*1*, Step 1.*b* are the same fuel spacers referenced in Section 9.1.1, Step 9.b. Fuel spacers may be placed below the assembly, above the assembly or both depending on the length of fuel assemblies to be loaded. For consistency, the term "bottom fuel assembly spacers" is revised to state "fuel spacers."

Response to Part 3

There are no requirements for fuel spacers under 10 CFR Part 72. Structural, confinement, thermal, shielding and criticality functions are attributed to the dry shielded canister (DSC) in the UFSAR. The spacers are located inside of the confinement boundary and are variably-sized depending on the site- specific fuel assembly length, control components, cavity length, and accounting for thermal expansion as to not affect the confinement function provided by the DSC shell assembly. Since the spacers provide an improved conduction path and add material for increased shielding at the top or bottom of the fuel assemblies, they do not have any adverse effect on the thermal or shielding functions of the DSC and are consistent with the design basis. Fuel spacers do not perform any structural design functions. They replace the void at the top and bottom of the fuel assembly to reduce the axial gap between the fuel assembly and DSC cavity.

In addition, based on a follow-up discussion during a meeting held via telephone with NRC staff on May 1, 2019, additional clarification has been added to include the materials of construction for the fuel spacers to demonstrate that they will not lead to adverse reactions during loading operations. The materials of construction for the fuel spacers consist of either 304 stainless steel, or in the case where weight is a concern, aluminum B209 Type 1100 or 6061 for aluminum spacers (solid blocks with material removed to create shallow drain slots to ease vacuum drying operations). These aforementioned materials are currently utilized within the DSC as either shell material or basket material, and are added to UFSAR Table 8-1, which defines the EOS-DSC materials. Their compatibility with loading operations, including immersion in the spent fuel pool, is evaluated in UFSAR Section 8.2.5.1 for aluminum, and UFSAR Section 8.2.5.2 for stainless steel. The effect of flammable gas generation when performing welding operations is addressed for both materials in UFSAR Section 8.5, and years of operating experience demonstrate that galvanic coupling between the stainless steel and aluminum has not been an issue, and carbon steel to aluminum is an even closer coupling on the galvanic scale, and therefore even less volatile. Additionally, hydrogen generation is closely monitored during the operations procedures as described in TS Section 5.4 and UFSAR Section 9.1.3.

No particular function is attributed to the fuel spacers in the UFSAR *under Part 72 storage operations*; therefore, the drawings for the fuel spacers are not provided in the UFSAR as they are not part of the licensing basis.

Application Impact:

UFSAR Section 9.1.1 *was* revised *as described in the response in Amendment 1 Rev 3*.

UFSAR Table 8-1 has been revised as described in the revised response.